Piperine phytosomes for bioavailability enhancement of domperidone

Nayyer Islam[1], Muhammad Irfan[1], Talib Hussain[2], Maria Mushtaq[3], Ikram Ullah Khan[1], Abid Mehmood Yousaf[2], Muhammad Usman Ghori[4], Yasser Shahzad[2,*]

[1]Department of Pharmaceutics, Faculty of Pharmaceutical Sciences, Government College University Faisalabad, Faisalabad, Pakistan
[2]Department of Pharmacy, COMSATS University Islamabad, Lahore Campus, Lahore, Pakistan
[3]Faculty of Pharmaceutical Sciences, University of Sargodha, Sargodha, Pakistan
[4]Department of Pharmacy, School of Applied Sciences, University of Huddersfield, UK

***Correspondence**

Dr. Yasser Shahzad
Assistant Professor of Pharmacy
COMSATS University Islamabad, Lahore Campus
Lahore, Pakistan
Email: y.shahzad@live.com

ABSTRACT

The markedly low oral bioavailability of domperidone (anti-emetic drug) is associated with rapid first-pass metabolism in the intestine and liver. To counteract such affects, there is a need to devise a strategy to enhance absorption and subsequently bioavailability. Thus, the current study was aimed at synthesizing phytosomes consisting of phosphatidylcholine and piperine (a P-glycoprotein inhibitor). Phytosomes were prepared by salting-out method. The developed phytosomes were extensively characterized for size, zeta potential, polydispersity index, entrapment efficiency (EE %), infrared spectroscopy, X-ray diffraction, *in-vitro* drug release, ex-vivo permeation, *in-vivo* pharmacokinetic and toxicity. The engineered formulations of phytosomes with piperine exhibited a significant improvement in oral bioavailability of domperidone (79.5%) in comparison with the pure drug suspension under the same conditions. Pharmacokinetic parameters such as maximal plasma concentration (C_{max}) and the plasma concentration (estimated from area under the curve; AUC) of domperidone have been greatly increased relative to drug alone. The improved drug absorption was attributed to inhibition of P-glycoprotein transporter. The findings of current research work suggest that the optimized phytosomes based drug delivery containing phytochemicals as bioenhancers have the potential to improve bioavailability of poorly bioavailable drugs that are substrate to P-glycoprotein.

Keywords: Piperine, domperidone, phospholipid, phytosomes, P-glycoprotein, bio-enhancers

1. Introduction

The oral route is by far the most preferred way of administering drugs (Mehmood et al., 2020). The desired pharmacological response is dependent on the bioavailability of drug, which is generally linked with relative solubility and permeability of oral drugs (Zhang et al., 2018). The oral drug absorption is highly unpredictable among individuals owing to the physiological variability (Chai et al., 2017). The pharmacokinetics and drug metabolism are regarded as key determining factors, playing a significant role in designing safe and effective dosage forms. Besides bioavailability challenge, another serious implication that could results in sub-optimal drug-plasma concentration is the intense metabolism of CYP450 enzymes or efflux transporter-like P-glycoprotein (P-gp) at the site of action. Higher drug doses are often recommended to achieve therapeutic response; however, this comes at the cost of increased side effects. Given that bioavailability of drugs could possibly be enhanced by inhibiting metabolism and efflux transporters through use of natural bio-enhancers, thereby reducing the side effects (Gerber et al., 2018).

Domperidone (DPD) is an anti-emetic drug, which is used to treat nausea and vomiting by increasing gastrointestinal motility (Chai et al., 2017). The reported oral bioavailability of DPD is circa 15-20%. The low oral bioavailability of DPD is related to drug-metabolizing enzymes (CYP3A4) and efflux transporters (P-pg) (Grube and Jedlitschky, 2020). Despite being an effective anti-emetic drug, the use of DPD is hampered owing to its reduced bioavailability, which can be mitigated through use of novel formulation strategies.

Phytosomes are nano-size carriers, providing new opportunities to enhance bioavailability of drugs (Lu et al., 2019). The interaction between natural ingredients and phospholipids can be used for therapeutic fortification. Phytosomal drug delivery systems have superior functionalities (monodisperse, more surface area, small size) than conventional dosage forms (Bhise et al., 2019). Unlike liposomes and lipid emulsions, the phytoconstituents are part of the vesicular membrane of phytosome, thus help phytocomponents to pass through the cell membranes and reach the target site or receptor (Hoque et al., 2021). This property makes them attractive carriers for active pharmaceutical ingredients in comparison with the conventional counterparts. Moreover, the bioavailability of many herbal extracts has been improved through phytosomal carriers (Karpuz et al., 2020). The presence of phospholipids in phytosomes makes them an ideal candidate to carry

hydrophilic as well as lipophilic drugs. The cell-membrane-like composition of phospholipid molecules helps them to permeate through physiological cell membranes easily. Hence, Phytosomes can appropriately decrease absorption and bioavailability related issues of drugs (Zhang et al., 2019). Likewise, in the case of DPD, phytosomes might facilitate the absorption and permeation through the membranes of intestinal epithelial cells.

Moreover, the permeability of drugs has been improved by the co-administration with bio-enhancers (Peterson et al., 2019). Thus, to improve the oral bioavailability of drugs, various types of bio-enhancers are being used. The natural bio-enhancers can potentiate the pharmacological effects of drugs, through inhibiting intestinal and hepatic efflux transporters, other multidrug resistance proteins, and drug-metabolizing enzymes, consequently, increases the bioavailability of drugs at very low concentrations. For instance, piperine (Lee et al., 2018), ginger resin (Markam et al., 2019) and glycyrrhizic acid (Selyutina and Polyakov, 2019) have successfully been used to increase the bioavailability of various drugs. Piperine (PPR), a golden yellow and needle shaped alkaloidal material derived from black pepper, has been documented to inhibit the CYP3A4 drug-metabolizing enzyme and plays an important role in drug absorption and disposition (Ren et al., 2019). Ginger, the rhizome of *Zingiber officinale* contains 6-gingerol and 6-shogaol, is commonly used for the prevention of diarrhea and other stomach disorders (Simon et al., 2020, Nikkhah Bodagh et al., 2019). Another natural bioenhancer, glycyrrhizic acid (active constituent of the roots of Licorice) comprises hydrophobic and hydrophilic regions in its structure. In aqueous solutions, GA can form micelles. The use of GA as a carrier can improve the therapeutic actions of drugs (Jin et al., 2020). However, bio-enhancers with a pro-kinetic property (function on gut motility) might not be the right candidates to improve DPD bioavailability, thus PPR was chosen for this research work (Feng et al., 2014).

PPR is extracted from black pepper (*Piper nigrum*) or long pepper (*Piper longum).* PPR can modulate the functions of metabolic enzymes and drug transporters. PPR inhibits the intestinal efflux transporter (P-gp) and metabolizing enzyme CYP3A4, thus, changing drug absorption and disposition pattern in the body (Hussaarts et al., 2019). The low oral bioavailability of DPD is linked with low absorption due to efflux transporters and high first-pass metabolism, thus making it a suitable candidate to load in phytosomes along with PPR.

Here we examined the effects of natural bio-enhancer on oral permeation and bioavailability of DPD using *in vitro* and *in vivo* models. Phytosomes loaded with PPR and DPD

were prepared and extensively characterized using various analytical tools such as Fourier transform infrared spectroscopy (FTIR), powder X-ray diffraction (PXRD), size, charge, entrapment efficiency (EE %) and *in-vitro* drug release. Influence of efflux receptors on DPD uptake was also studied. Finally, the phytosomes were subjected to *in-vivo* pharmacokinetic and cytotoxicity studies.

2. Materials and methods

2.1.Materials

Domperidone was obtained from Batala Pharmaceuticals, Pakistan. Phospholipon® 90H was a gift sample of Lipoid GmbH, Germany. Piperine, n-hexane, and ethanol were procured from Sigma-Aldrich (China). Caco-2 cells, Mock-MDCK cells, and MDR-MDCK cells were obtained from Sigma Aldrich, China. Acetonitrile was used of chromatographic grade (Merck, Germany). All chemicals used were of analytical grade and were used as received.

2.2.Preparation of phytosomes

Phytosomes were prepared by dissolving DPD, phosphatidylcholine (PC), and PPR in ethanol and the mixture was blended for one hour in a round-bottom flask as depicted in Figure 1. Then the flask was attached with a rotary evaporator (Rotavapor R 300, Buchi Labortechnik AG) and the solution was concentrated to 3 – 4 mL at 40 °C under reduced pressure. Subsequently, n-hexane was added to the concentrated solution, followed by standing overnight to precipitate. The precipitates were obtained by filtration and washed with cold n-hexane. The dried residues were collected and sieved through a 200-mesh screen. The resultant phytosomes were transferred into a glass bottle and stored in a desiccator for further evaluations (Freag et al., 2013). The composition of phytosome formulations is illustrated in Table 1.

Table 1 Composition of phytosomes formulations

Formulation composition	**PP1**	**PP2**	**PP3**
Domperidone (mg)	100	100	100
Piperine (mg)	1	2	3
PC (mg)	100	100	100
Ethanol (mL)	30	30	30

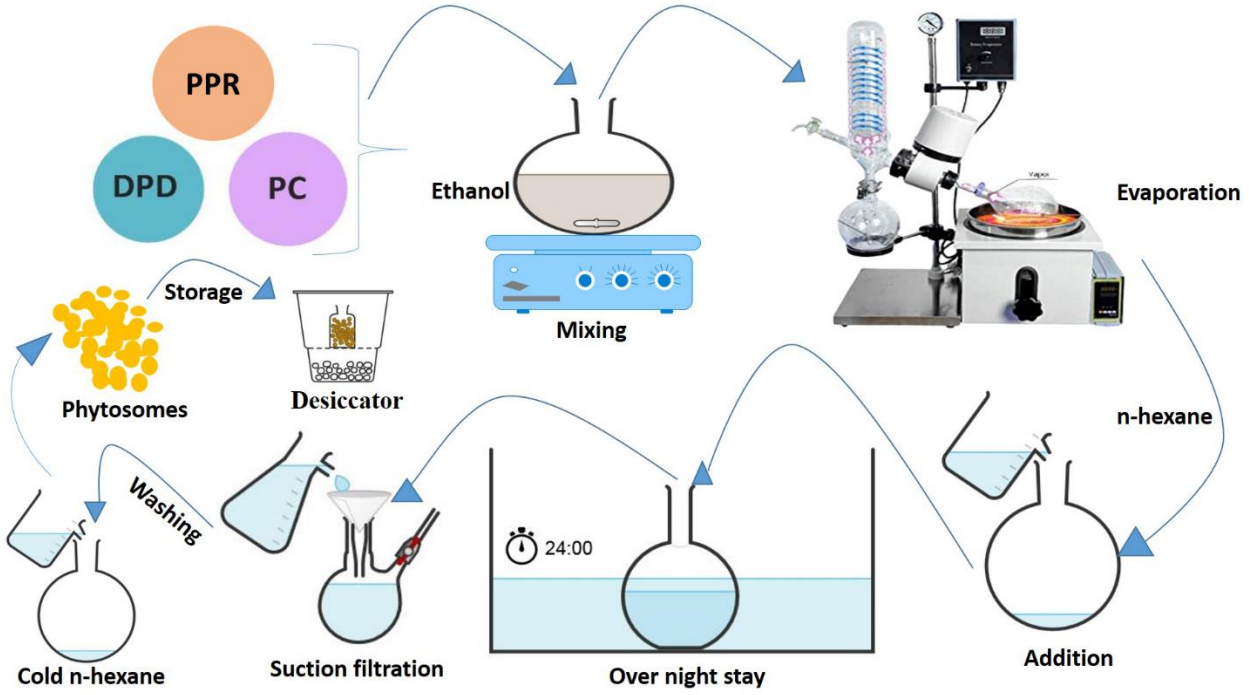

Figure 1. Schematic diagram of manufacturing process of phytosomes.

2.3.High-performance liquid chromatography (HPLC) analysis of DPD

DPD analysis was conducted through HPLC (Shimadzu HPLC, LC-2010AHT). HPLC was equipped with solvent delivery unit LC-20AD. The HPLC conditions were set at a flow rate of 1 mL / min and the UV–Visible detector at 284 nm. A C18 column (4.6 × 150 mm, 5µm particle size) was used for drug elution. The column oven temperature was set at 25 °C. The mobile phase was consisted of acetonitrile and distilled water at 60:40 v/v ratio. The orthophosphoric acid (pH 2.5) was used to change the pH of the mobile phase. In HPLC port, 20 µL samples were injected for analysis. To measure the quantity of the drug, the retention time and peak area of the standard and samples were noted.

2.4.Characterizations

2.4.1. Particle size, polydispersity index and zeta potential

The z-average mean particle size, polydispersity index (PDI) and zeta potential of phytosomes were measured using Zetasizer Nano-Z (Malvern Instruments, UK). Each sample was analyzed in triplicate and the results are reported as mean ± standard deviation.

2.4.2. Entrapment efficiency (E.E.)

The entrapment efficiency of DPD in phytosomes was estimated using HPLC following a previously mentioned method with slight modification (Tetyczka et al., 2019). Briefly, phytosomes were disrupted with methanol and mounted in centrifuge machine (Compact, Thermo-Fisher Scientific, Waltham, Massachusetts, USA) and centrifuged for 30 min at 10062 × g. The supernatant was taken and analyzed at HPLC after suitable dilutions with mobile phase. The entrapment efficiency (%) was determined using the following equation.

$$\text{EE (\%)} = \frac{\text{Total drug - Entrapped drug}}{\text{Total drug}} \times 100$$

2.4.3. Fourier transform infrared spectroscopy (FTIR)

FTIR spectra of PC, DPD, PPR, and PP3 were obtained through Fourier transform infrared spectrophotometer with attenuated total reflectance (ATR) interface (FTIR-Cary 360, Agilent technologies, USA). FTIR Spectra were recorded in the spectral range of 500 – 4000 cm^{-1} at the resolution of $2cm^{-1}$.

2.4.4. X-ray diffraction studies (XRD)

X-ray diffraction patterns for DPD, PP2, and PP3 were obtained using advanced XRD diffractometer (D8 Advance, Bruker, Massachusetts, USA) equipped with a CuKα radiation source operating at 30 mA and 40 kV. Data was recorded from 2θ angle of 10° to 60° at a step width of 0.02° and scanning speed of 4°/min.

2.4.5. Uptake studies

Uptake studies were conducted as mentioned previously with slight modification (Huo et al., 2013). Caco-2 cells at a density of 5×10^5 cells/well were cultivated for 15 days on a 24-well plate. Monolayers of Caco-2 cells were washed with HBSS (145 mM NaCl, 3 mM KCl, 1 mM $CaCl_2$, 0.5 mM $MgCl_2$, 5 mM D-glucose and 5 mM MES). Pre-incubation (at 37 °C for 15 min) was made before the start of experiments. DPD was dissolved in HBSS (pH 6.0). The uptake experiments were conducted by incubating domperidone (20 µM) alone and a combination of domperidone (20 µM) and verapamil (200 µM) on Caco-2 cell monolayers. Subsequently, the medium of cell layers was removed completely. The uptake of DPD was terminated by washing with cold HBSS. Triton®

(0.3 mL 0.1%) was used for lysing monolayers of Caco-2 cells. The concentration of DPD in cell lysate was calculated.

2.4.6. Bidirectional transport studies

Bi-directional transport experiments were conducted to establish the receptor (P-pg) mediated transport of DPD. A slightly modified method was used to study trans-epithelial transport (Huo et al., 2013). In 24-well, Mock- MDCK cells and MDR1–MDCK cells were seeded for 3 – 5 days. The cell layer integrity was tested using a trans-epithelial / endothelial electrical resistance (TEER) experiment (EVOM2™ equipment). As an acceptance criterion, TEER ≥ 350 Ωcm^2 was used. Digoxin was used as a P-gp (aq) probe substrate (positive control). Digoxin (20 µM) already dissolved in HBSS buffer (pH 7.4), was placed on the apical and basal sides of the monolayer in HBSS (300 µL). The aliquot was drawn at predetermined time intervals of incubation (0.5, 1.0, 2.0, and 3.0 h) and the medium was replenished with fresh buffer. In the DPD efflux inhibition assay, verapamil (200µM) was used as a P-gp inhibitor. The DPD (20 µM) and verapamil (200 µM) were dissolved in HBSS buffer (pH 7.4). The inhibitor's solution was placed on both sides of Mock- MDCK cells and MDR1–MDCK cell layers. Uptake of DPD was terminated by washing both sides of the cell monolayer with cold HBSS. Monolayers were lysed with Triton® to measure the intracellular accumulation of DPD.

2.4.7. Animal experiments

The animal study protocols were reviewed by the institutional animal ethical committee and approved by the Institutional Review Board (IRB), Government College University Faisalabad. (Ref No. GCUF/ERC/2068, Study No. 19668, IRB No. 668, Dated 05-09-2019). Male Wistar rats, weighing between 200 and 250 g, were obtained from animal house. Animals were kept in normal standards of temperature, humidity, and daylight. Food and water were given ad libitum. The rats fasted overnight prior to experiment.

2.4.7.1.Ex-vivo membrane permeation studies and drug quantification

Permeation study of phytosomes was conducted in the everted gut sac of male Wistar rat. The facts established based on DPD intestinal absorption, can be used to determine the efficiency of PPR as P-gp inhibitor. Rats were anesthetized with chloroform, then the small intestine was removed. The isolated small intestine of the rat was washed with Tyrode buffer solution (pH 7.4) to remove wreckages and then placed in an oxygenated Tyrode buffer solution. The small segment (5 cm) of the ileum was cut and everted on the glass rod. The everted gut was clumped from one

end and filled with 500µL Tyrode buffer. Then second end of the gut was sealed and clumped, and the gut sac was placed in the test solution containing 20 µM DPD with or without 200µM verapamil, maintained at 37 ± 0.5°C. The samples were collected at predetermined times intervals (0, 20, 40, 60, 80,120 minutes) and drug permeated across the intestinal membrane was evaluated using the RP-HPLC method (LC-2010AHT, Shimadzu, Japan) (Tetyczka et al., 2017). Permeability studies were conducted for pure DPD, verapamil mixed with DPD, and phytosomes loaded with DPD and PPR.

2.4.7.2.Bioavailability study in rats

The rats were randomly divided into three treatment groups, namely A, B, and C with 6 rats in each group. The rats were fasted for 12 h before the experiments. Group A, B and C were treated with DPD (10 mg/kg), PP3 (DPD dose at 10 mg/kg) and DPD + verapamil phytosome (DPD dose at 10 mg/kg), respectively. The three groups of rats were administered a single oral dose through an oral gavage. To evaluate the pharmacokinetic parameter, the blood samples were collected and stored in heparinized vials at the predetermined time intervals of 0, 0.25, 0.5, 1, 2, 3, 4, 6, 8, 10, 12, and 24 hours. The plasma obtained after centrifugation (at 1610 × g for 10 min) was kept at -20°C for further analysis. The plasma DPD concentrations were determined through reverse phase HPLC method with little modification. Briefly, all plasma samples were centrifuged at 2516 × g for 5 min before analysis. The samples containing 200 µL of the plasma and 200 µL of acetonitrile, were shaken and centrifuged at 2516 × g for 5 min. The supernatant (200 µL) was taken and purged with nitrogen gas which was further reconstituted with a 50 µL mobile phase (40% acetonitrile and 60% of 0.1 M phosphate buffer of pH 3.9). A volume of 20 µL of the prepared samples was injected into RP-HPLC (Shimadzu, Japan), which was analyzed at wavelength of 284 nm and flow rate 1 mL/min. The retention time of DPD and internal standard (propranolol) was found to be 5.6 and 7.5 min. respectively (Jin et al., 2013).

2.4.8. Cytotoxicity assay

MTT assay was employed to investigate the cytotoxicity of phytosomes on Human intestinal epithelium Caco-2 cells. The cells were seeded on 96-well plates with cell density of 1×10^5 cells/well. Then phytosomes (concentration of 50 µg/50 µL) was introduced in well plates and incubated at 37 °C for 24 h. To perform cytotoxicity assay, 20 µL of MTT (5mg/mL stock solution) was added to each well and incubated at 37 °C for further 4 h. The water-insoluble formazan

crystals were formed from yellowish-water-soluble MTT solution. The remaining yellowish water-soluble MTT solution was removed from all wells and 150 µL of DMSO was put into each well to dissolve formazan crystals. The absorbance was measured by a microplate reader **(**EnSight®, PerkinElmer) at 570 nm. The absorbance of controlled cells was taken at the same wavelength (Sabapati et al., 2019). The assay was carried out in triplicate.

$$\text{Cell viability (\%)} = \frac{\text{Absorption of test}}{\text{Absorption of control}} \times 100$$

2.4.9. Statistical analysis

The experimental data was presented as the mean and standard deviation. The Student t-Test was carried out using Origin 8.5 (OriginLab, USA) software to evaluate the difference in results and the $P < 0.05$ was considered significant.

3. Results and discussion

3.1. Particle size, zeta-potential, polydispersity index and entrapment efficiency (E.E.) of phytosomes

The results of particle size, polydispersity index, zeta-potential, and entrapment efficiency of PP1, PP2, and PP3 are shown in Table 2**.** The phytosomes size was ranged between 150 to 170 nm, while the narrow particle size distribution was confirmed from low polydispersity index values. The average zeta potential of phytosomes was ranged from -20.6 to -26.4, thus indicating good stability of phytosomes by reducing the tendency of phytosomes to agglomerate (Souto et al., 2019). The stability indicating zeta potential values were associated with the presence of PC in the formulations. The entrapment efficiency of phytosomes was high owing to the lipophilicity of DPD and PC, hence, optimal choice of PC and DPD has warranted the high entrapment efficiency (Perteghella et al., 2020).

Table 2. Particle size, zeta-potential, poly-dispersity index, and entrapment efficiency of developed phytosomes

Formulation	Particle size (nm)	PDI	Zeta potential (mV)	EE (%)
PP1	158.2± 1.1	0.142 ± 0.04	-20.6 ± 3.81	71.14 ± 0.29
PP2	163.4 ± 2.6	0.156 ± 0.01	-22.6 ± 1.76	80.67 ± 0.42
PP3	167.2 ± 4.2	0.160 ± 0.01	-26.4 ± 4.26	83.42 ± 0.17

3.2.FTIR spectroscopy

The interactions between DPD, PC, and PPR were investigated by FTIR studies as shown in Figure 2. For PPR, aromatic C-H stretching was found in the high frequency region at 2922 cm^{-1} and 2857 cm^{-1}. The symmetric and asymmetric stretching of C=C were found at 1627 cm^{-1} and 1606 cm^{-1}. The aromatic stretching of C=C (benzene ring) was found at 1582 cm^{-1} and 1436 cm^{-1}. The stretching of -CO-N was found at 1638 cm^{-1}. Further, the strong absorption peaks of PC were found at 2,854 cm^{-1} and 2,924 cm^{-1}. The carbonyl (C=O) group's stretching vibration was observed by peak appearing at 1,736 cm^{-1}. Furthermore, the presence of –CONH group in DPD was confirmed by N-H stretching at 3124 cm^{-1} and C=O stretching at 1690.30 cm^{-1}. The asymmetric C-H stretching and symmetric C-H stretching was appeared at 2932.28 cm^{-1} and 2812.61 cm^{-1}, respectively. The aromatic C-H stretching displayed its peak at 3010.26 cm^{-1}. In addition, no major variation was found in the IR spectrum of PP3 (Figure 2). The close analysis of all characteristic peaks and their corresponding wavenumbers demonstrated absence of any serious interaction between DPD and the excipients. However, the intensity of DPD characteristic peaks was attenuated probably because of entrapment within the vesicles.

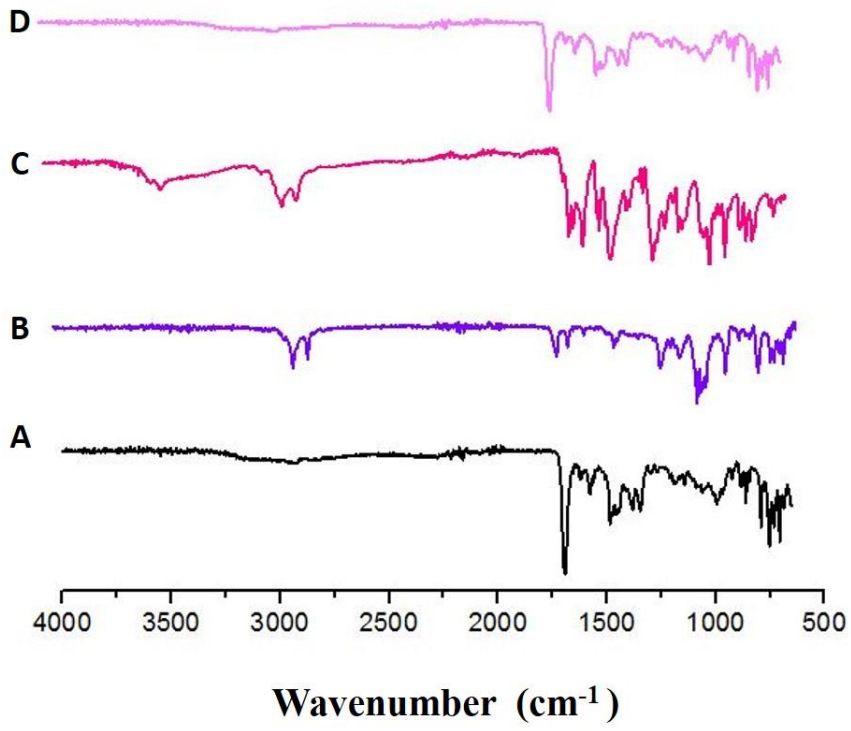

Figure 2 FTIR spectra of (A) DPD (B) PC (C) PPR (D) PP3.

3.3.XRD studies

The XRD patterns of DPD, PC, PPR and PP3 are illustrated in Figure 3. The crystalline nature of pure DPD was confirmed by the appearance of sharp diffraction peaks. Interestingly, the characteristic diffraction peaks of DPD were retained in the PP3 formulation, although with reduced intensity, thereby suggesting partial transformation of DPD from crystalline to amorphous form upon encapsulation within the vesicles. Moreover, the appearance of diffraction peaks in PP3 could also be related to the diffraction peaks of PPR and the single sharp diffraction peak of PC. The XRD results complement our FTIR outcomes, thus confirming a partial conversion of crystalline DPD into amorphous form.

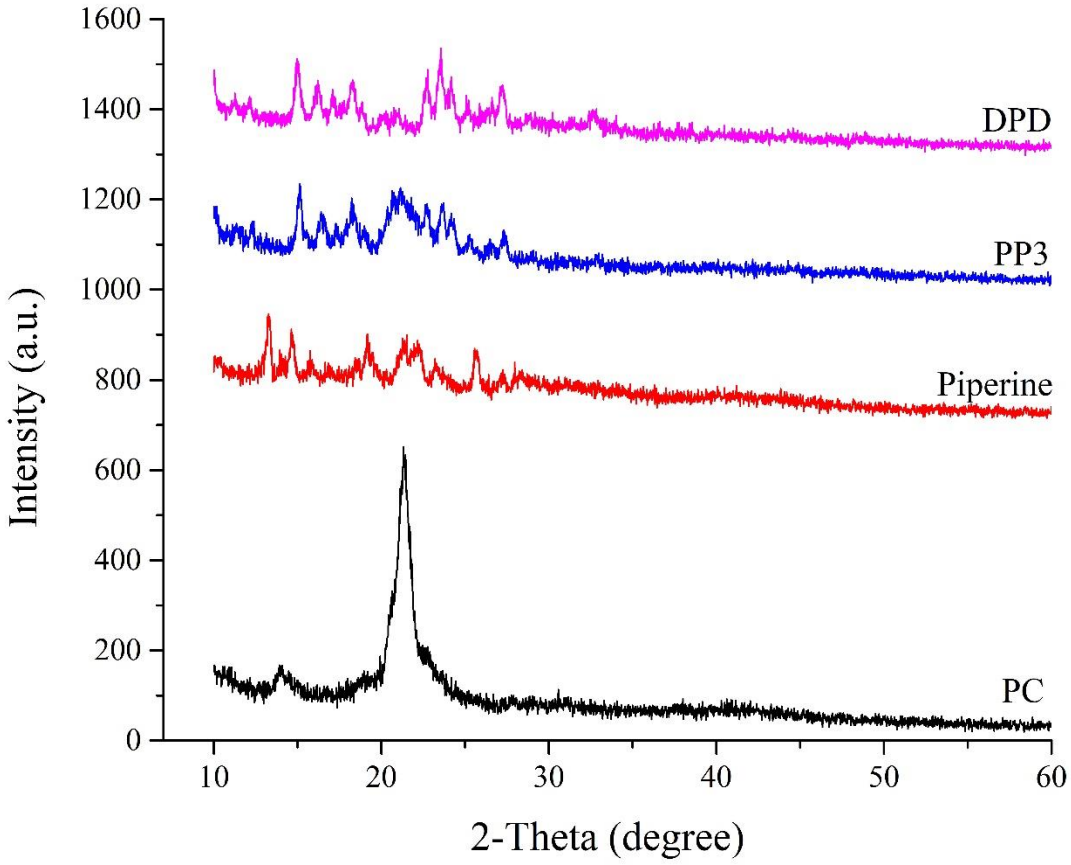

Figure 3. XRD patterns of formulation and ingredients.

3.4.Uptake studies

The membrane efflux transporters could be involved as a barrier in drug transportation (Vertzoni et al., 2019). To investigate the involvement of drug transporter, potent inhibitor was added in uptake studies. The relevant accumulation of DPD in Caco-2 cells is presented in Figure 4. It has been evinced that the epithelium cells resisted the DPD transport into the cells. The amount of cellular uptake was increased after incubation with verapamil. The interaction between DPD-P-gp inhibitors and Caco-2 cells were induced. The concentration of DPD in cells was enhanced by the presence of verapamil (Yoshizato et al., 2012). Results suggested that inhibition of efflux transporters (P-gp) increased the intracellular concentration of drugs. The improved uptake of DPD was attributed to the presence of transporter such as PEPT1 on the Caco-2 cells which possibly

had facilitated the absorption of DPD (Vaessen et al., 2017). The intestinal absorption of DPD was further explored to understand the uptake mechanism in Caco-2 cells through bidirectional studies.

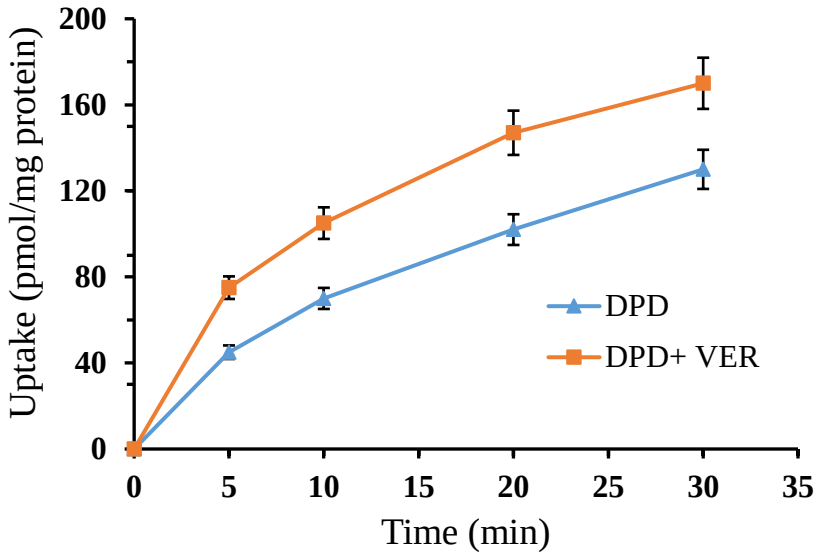

Figure 4. Uptake of DPD by Caco-2 cells with and without verapamil.

3.5.Bi-direction studies

The bi-directional analysis was performed to track the cells involved in the transport of DPD. Digoxin demonstrated vector transfer through the Mock–MDCK and MDR1–MDCK cell monolayers (Figure 5A & 5B). TEER value was found greater than 350 Ωcm^2 in all cell lines. The amount of the efflux was about double that of the inflow. In the presence of verapamil, the net efflux ratio was decreased. The transcellular transport of DPD did not indicate any vector movement through the Mock-MDCK cells (Figure 5C). P-gp mediated efflux transport of DPD was confirmed by the basolateral-to-apical trans-epithelial transport in MDR1–MDCK cells (Figure 5D). The DPD basolateral-to-apical (B-A) transport was 2 times higher than apical-to-basolateral (A-B) transport. The transport of DPD was decreased from B-A in the presence of verapamil. Results showed that inhibition of P-gp-mediated efflux by verapamil enhanced the aggregation of DPD in MDR1–MDCK cells. Digoxin is P-gp substrate thus used as a probe (positive control) to validate the test. Digoxin exhibited vectorial transport in MDR1–MDCK cells. Verapamil demonstrated inhibitory effects by reducing the efflux transport of digoxin. The basal-to-apical transport of DPD was significantly greater than that of apical-to-basal transport. The net efflux value was almost double the influx value. The efflux of DPD was inhibited through

verapamil. It was certainly established that the DPD was a P-gp substrate (Dan et al., 2002). Thus, by inhibiting the P-gp through a reasonable natural inhibitor, the treatment efficiency of DPD can be enhanced.

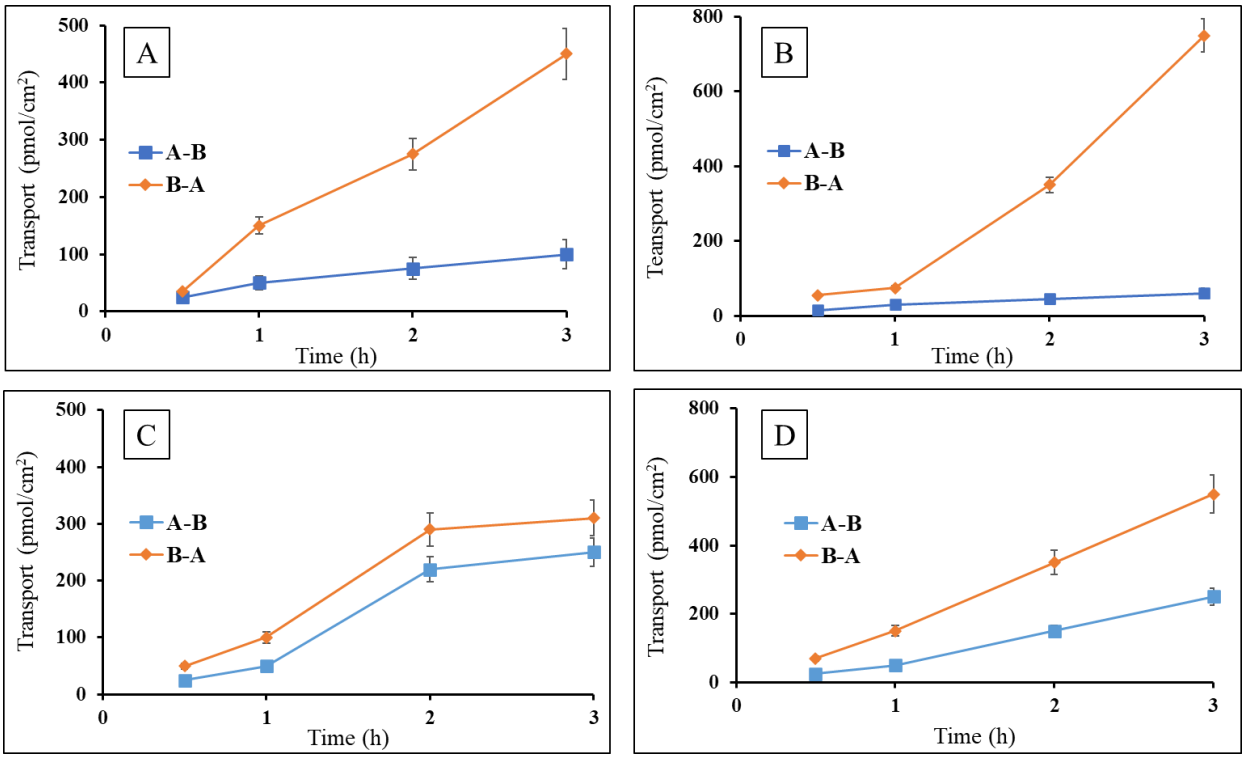

Figure 5. Bi-directional transport of digoxin across Mock-MDCK (A) and MDR1–MDCK (B). Bi-directional transport of DPD across Mock-MDCK (C) and MDR1–MDCK (D).

3.6. *Ex-vivo* permeation study

To determine the level of intestinal absorption, *in vitro* everted gut sac absorption model was used, and the results are presented in Figure 6. The concentration of pure DPD permeated through the intestine was found to be 0.96 ± 0.03 µg/5cm, while the amount of drug permeated with verapamil formulation was 1.87 ± 0.04 µg/5cm. However, the highest permeability was achieved with phytosomes, i.e., 2.23 ± 0.02 µg/5cm. Moreover, it was also observed that the diffusion of crystalline DPD was enhanced persuasively over time. The diffusion of DPD was increased in dose-dependent and time-dependent fashion. Thus, high solubilizing properties of PC along with

p-gp inhibiting activities of PPR collectively enhanced the permeation of DPD. Moreover, PC can interact with the biological membranes, thus facilitating the absorption of DPD through the GIT. The high concentration of PC reduces the release of drug from dermal layers thus show sustain release behavior at high concentration. It is observed that the efficiency of phytosomes is appreciably increased at the 1:1 ratio of DPD and PC. When the concentration of PPR and PC are increased in the formulations, the drug permeation is increased proportionally as shown by PP2 and PP3. The concentration of PPR in phytosomes was directly proportional to the extent of drug diffusion. The diffusion rate of DPD was increased with increasing the concentration of PPR. PPR at a concentration of 1% w / w did not demonstrate a noticeable improvement at 15 and 30 minutes, however, the diffusion improved significantly at 45, 60, and 120 minutes (data not shown). Moreover, PPR at 2% (data not shown) and 3% w/w concentration dramatically enhanced the diffusion of DPD at 45 and 60 minutes, with later had slight superior results, thus PP3 phytosome (3% PPR concentration) was chosen for further studies. The combined use of PC and PPR in phytosomes contributed a better performance in terms of permeation than to results of separately used ones. Hence, significance of these results can be evaluated based on comparison with the permeation results of verapamil (potent inhibitor of p-gp). Permeation results of PP3 are consistent with the results of verapamil, implying good p-gp inhibitory properties of PPR. Thus, PPR can be used safely for the enhancement of bioavailability of DPD. The role of PPR as a P-gp inhibitor was consistent with the reported study of Katiyar and co-workers in which the permeability of rapamycin was increased several folds in the presence of PPR (Katiyar et al., 2016). The findings of the intestinal sac offered a clear insight into the impact of P-gp on the intestinal absorption of DPD. The intestinal absorption of DPD was changed by the inhibition of P-gp activity. The site of interaction of DPD and P-gp was the intestine. P-gp is extensively expressed in the intestine and plays a vital role in mitigating oral bioavailability by efflux activity and in reducing the therapeutic effects of different medicines.

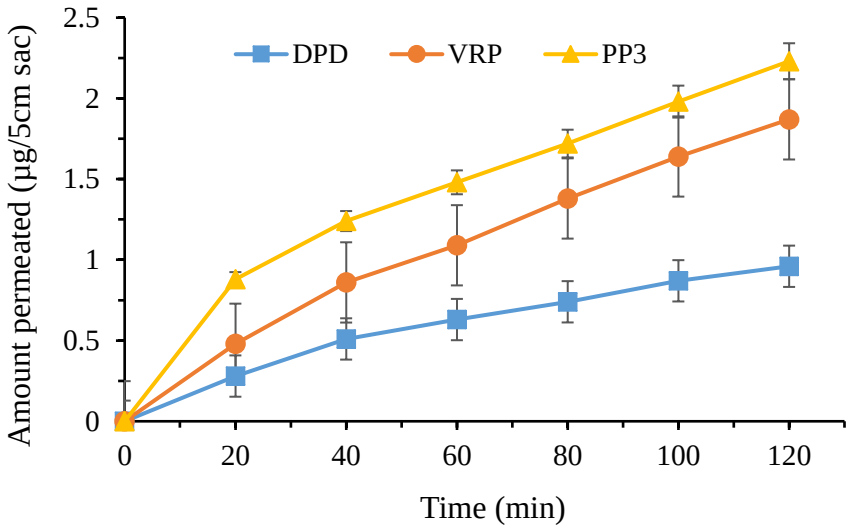

Figure 6. *Ex vivo* permeation studies.

3.7. *In vivo* study of DPD in rats

The study was carried out to gain valuable information about the optimized level of drug required for therapeutic response by evaluating the impact of P-gp inhibitors on DPD intestinal absorption (Figure 7). The significance of verapamil as an efflux transporter inhibitor of P-gp through improved absorption of co-administration drugs is well established. In the current study, improved pharmacokinetic profile of DPD in the presence of verapamil was observed in the form of 125 % rise in AUC (Table 3). However, the elimination of DPD remains relatively constant, indicating the existence of inhibitor and receptor association. The treatments were well tolerated by all rats and there were no cases of serious adverse reactions during the study period. The standard pharmacokinetic parameters for pure DPD group A (10 mg/kg), PP3 group B (DPD dose at10 mg/kg), and DPD+verapamil group C (DPD dose at 10 mg/kg) groups are listed in Table 3. The significantly improved pharmacokinetic profile of group B in comparison to control group A ($P < 0.05$), reflected by the difference in values of C_{max} and $AUC_{0–24}$ as depicted in Table 3. DPD, a substrate to P-gp transporters, intestinal absorption is achieved through passive diffusion instead of active transport. Hence, increased bioavailability is attributed to the combined impact of inhibition of CYP-group metabolizing enzymes and inhibition of P-gp efflux transporter. The acclaimed potential of PPR as drug efflux pump inhibitor (P-gp efflux transporter) along with PC in changing membrane mechanics and permeation properties, resulted in the form of increased

passive diffusion of DPD (Jhanji et al., 2019). The pharmacokinetic results of the verapamil treated group and the PPR treated group are in close agreement, suggesting the effectiveness of PPR as P-gp inhibitor. DPD phytosomes have offered improved pharmacokinetics, augmented metabolic stability, amplified membrane permeability, and boosted bioavailability (Hafez et al., 2020).

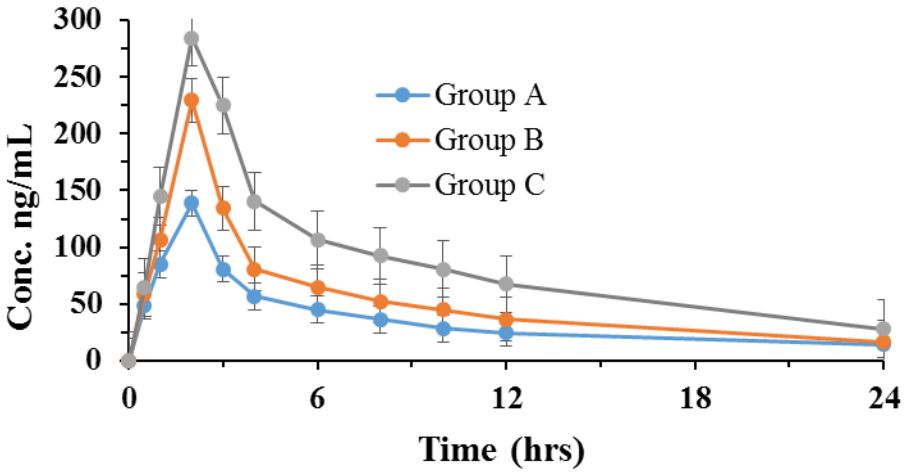

Figure 7. The plasma concentration-time curve of DPD in rats after oral administration.
Note: Data are presented as mean ± standard deviation (n = 6). Group A represents DPD treated as control; Group B represents PP3, and Group C represents DPD+verapamil treated.

Table 3 Pharmacokinetic parameters of DPD in Group A, Group B, and Group C

Pharmacokinetic parameters	Group A (DPD)	Group B (PP3)	Group C (DPD+verapamil)
C_{max} (ng/mL)	138.6 ± 4.6	229.3 ± 6.3*	284.4 ± 11.4*
T_{max} (h)	2.0 ± 0.1	2.0 ± 0.1	2.0 ± 0.2
$AUC_{0\text{-}24h}$ (ng/mL.h)	1462.9 ± 32.9	2626.1 ± 43.5*	3293.6 ± 42.9*
$t_{1/2}$ (h)	4.4 ± 0.04	5.5 ± 0.1	5.8 ± 0.1

Note: Data are presented as mean ± standard deviation (n = 6). *P < 0.05 statistically significant vs control.

3.8. Cytotoxicity assay

The comparative cytotoxicity analysis was performed for control, plain phytosomes, and DPD loaded phytosomes (500 µg/mL) to evaluate their compatibility in living cells (Figure 8). For

control cells, the viability of the cells was considered 100%. The percentage survival of cell lines was found above 90% as shown in Figure 8. No signs of cytotoxicity to human intestinal epithelium Caco-2 cells observed by DPD phytosomes (500 µg/mL). The MTT evaluates the metabolic behavior of the cells through analyzing viability of cells associated with the cytotoxicity by phytosomes. The developed phytosomes have presented a safe profile at high concentration. The actual loading of DPD in phytosomes is even less than the tested concentration. Therefore, it is plausible to say that the prepared phytosomes were safe to be used in humans.

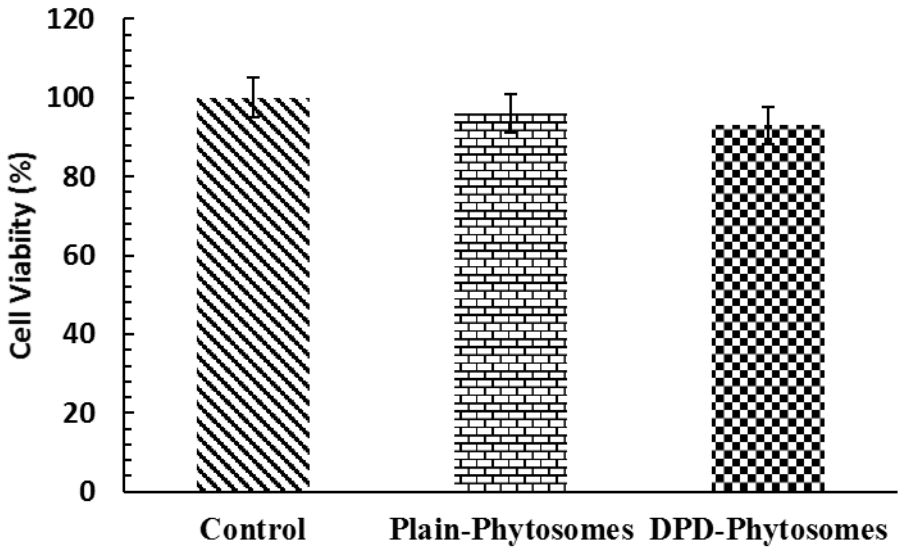

Figure 8. Cell viability Human intestinal epithelium Caco-2 cells after exposure to plain phytosomes and DPD loaded phytosomes for 24h.

4. Conclusions

DPD loaded phytosomes has been successfully developed and evaluated for bioavailability enhancement. Phytosomes (PP3) have demonstrated significant improvements in DPD absorption and bioavailability owing to inhibition of P-gp by PPR in the intestine and liver. PPR in conjunction with phosphatidylcholine has improved the oral pharmacokinetics of DPD. The involvement of bio-enhancer in developed phytosomes suggests a roadmap for the improvement of oral absorption of poorly bioavailable drugs. Consequently, bio-enhancers could be used in combination with other medicines to boost bioavailability in the future. Clinical studies are required to evaluate the effects of receptors manipulation by lipid formulations and P.gp Inhibitors.

Further investigations are also required to get clear insight regarding long term medical complications associated with transporters inhibition.

Acknowledgements

The authors would like to acknowledge Faculty of Pharmaceutical Sciences, GC University Faisalabad for providing all the facilities to conduct the research work.

Conflict of interest

None declared.

References

BHISE, J. J., BHUSNURE, O. G., JAGTAP, S. R., GHOLVE, S. B. & WALE, R. R. 2019. Phytosomes: A Novel Drug Delivery for Herbal Extracts. *Journal of Drug Delivery and Therapeutics,* 9**,** 924-930.

CHAI, X., CHAI, H., WANG, X., YANG, J., LI, J., ZHAO, Y., CAI, W., TAO, T. & XIANG, X. 2017. Fused deposition modeling (FDM) 3D printed tablets for intragastric floating delivery of domperidone. *Scientific reports,* 7**,** 1-9.

DAN, Y., MURAKAMI, H., KOYABU, N., OHTANI, H. & SAWADA, Y. 2002. Distribution of domperidone into the rat brain is increased by brain ischaemia or treatment with the P-glycoprotein inhibitor verapamil. *Journal of pharmacy and pharmacology,* 54**,** 729-733.

FENG, X., LIU, Y., WANG, X. & DI, X. 2014. Effects of piperine on the intestinal permeability and pharmacokinetics of linarin in rats. *Molecules,* 19**,** 5624-33.

FREAG, M. S., ELNAGGAR, Y. S. & ABDALLAH, O. Y. 2013. Lyophilized phytosomal nanocarriers as platforms for enhanced diosmin delivery: optimization and ex vivo permeation. *Int J Nanomedicine,* 8**,** 2385-97.

GERBER, W., STEYN, J. D., KOTZÉ, A. F. & HAMMAN, J. H. 2018. Beneficial pharmacokinetic drug interactions: a tool to improve the bioavailability of poorly permeable drugs. *Pharmaceutics,* 10**,** 106.

GRUBE, M. & JEDLITSCHKY, G. 2020. ABC Transporters. *Encyclopedia of Molecular Pharmacology***,** 1-7.

HAFEZ, D. A., ELKHODAIRY, K. A., TELEB, M. & ELZOGHBY, A. O. 2020. Nanomedicine-based approaches for improved delivery of phyto-therapeutics for cancer therapy. Taylor & Francis.

HOQUE, M., AGARWAL, S., GUPTA, S., GARG, S., SYED, I., RUPESH, A., MOHAPATRA, N., BOSE, S. & SARKAR, P. 2021. 3.34 - Lipid Nanostructures in Food Applications. *In:* KNOERZER, K. & MUTHUKUMARAPPAN, K. (eds.) *Innovative Food Processing Technologies.* Oxford: Elsevier.

HUO, X., LIU, Q., WANG, C., MENG, Q., SUN, H., PENG, J., MA, X. & LIU, K. 2013. Enhancement effect of P-gp inhibitors on the intestinal absorption and antiproliferative activity of bestatin. *European Journal of Pharmaceutical Sciences,* 50**,** 420-428.

HUSSAARTS, K. G., HURKMANS, D. P., OOMEN-DE HOOP, E., VAN HARTEN, L. J., BERGHUIS, S., VAN ALPHEN, R. J., SPIERINGS, L. E., VAN ROSSUM-SCHORNAGEL, Q. C., VASTBINDER, M. B. & VAN SCHAIK, R. H. 2019. Impact of

Curcumin (with or without Piperine) on the Pharmacokinetics of Tamoxifen. *Cancers,* 11**,** 403.

JHANJI, R., BHATI, V., SINGH, A. & KUMAR, A. 2019. Phytomolecules against bacterial biofilm and efflux pump: An In silico and In vitro study. *Journal of Biomolecular Structure and Dynamics***,** 1-13.

JIN, N., LIN, J., YANG, C., WU, C., HE, J., CHEN, Z., YANG, Q., CHEN, J., ZHENG, G. & LV, L. 2020. Enhanced penetration and anti-psoriatic efficacy of curcumin by improved smartPearls technology with the addition of glycyrrhizic acid. *International Journal of Pharmaceutics,* 578**,** 119101.

JIN, X., ZHANG, Z. H., SUN, E., TAN, X. B., LI, S. L., CHENG, X. D., YOU, M. & JIA, X. B. 2013. Enhanced oral absorption of 20(S)-protopanaxadiol by self-assembled liquid crystalline nanoparticles containing piperine: in vitro and in vivo studies. *Int J Nanomedicine,* 8**,** 641-52.

KARPUZ, M., GUNAY, M. S. & OZER, A. Y. 2020. Liposomes and phytosomes for phytoconstituents. *Advances and Avenues in the Development of Novel Carriers for Bioactives and Biological Agents.* Elsevier.

KATIYAR, S. S., MUNTIMADUGU, E., RAFEEQI, T. A., DOMB, A. J. & KHAN, W. 2016. Co-delivery of rapamycin-and piperine-loaded polymeric nanoparticles for breast cancer treatment. *Drug delivery,* 23**,** 2608-2616.

LEE, S. H., KIM, H. Y., BACK, S. Y. & HAN, H.-K. 2018. Piperine-mediated drug interactions and formulation strategy for piperine: recent advances and future perspectives. *Expert Opinion on Drug Metabolism & Toxicology,* 14**,** 43-57.

LU, M., QIU, Q., LUO, X., LIU, X., SUN, J., WANG, C., LIN, X., DENG, Y. & SONG, Y. 2019. Phyto-phospholipid complexes (phytosomes): A novel strategy to improve the bioavailability of active constituents. *Asian journal of pharmaceutical sciences,* 14**,** 265-274.

MARKAM, R., BAJPAI, J. & BAJPAI, A. 2019. Synthesis of ginger derived nanocarriers (GDNC) and study of in vitro release of 5-amino salicylic acid (5-ASA) as an anti inflammatory drug. *Journal of Drug Delivery Science and Technology,* 50**,** 355-364.

MEHMOOD, Y., KHAN, I. U., SHAHZAD, Y., KHAN, R. U., KHALID, S. H., YOUSAF, A. M., HUSSAIN, T., ASGHAR, S., KHALID, I. & ASIF, M. 2020. Amino-decorated mesoporous silica nanoparticles for controlled sofosbuvir delivery. *European Journal of Pharmaceutical Sciences,* 143**,** 105184.

NIKKHAH BODAGH, M., MALEKI, I. & HEKMATDOOST, A. 2019. Ginger in gastrointestinal disorders: a systematic review of clinical trials. *Food science & nutrition,* 7**,** 96-108.

PERTEGHELLA, S., MANDRACCHIA, D., TORRE, M. L., TAMMA, R., RIBATTI, D., TRAPANI, A. & TRIPODO, G. 2020. Anti-angiogenic activity of uncoated-and N, O-carboxymethyl-chitosan surface modified-Gelucire® 50/13 based solid lipid nanoparticles for oral delivery of curcumin. *Journal of Drug Delivery Science and Technology,* 56**,** 101494.

PETERSON, B., WEYERS, M., STEENEKAMP, J. H., STEYN, J. D., GOUWS, C. & HAMMAN, J. H. 2019. Drug bioavailability enhancing agents of natural origin (bioenhancers) that modulate drug membrane permeation and pre-systemic metabolism. *Pharmaceutics,* 11**,** 33.

REN, T., YANG, M., XIAO, M., ZHU, J., XIE, W. & ZUO, Z. 2019. Time-dependent inhibition of carbamazepine metabolism by piperine in anti-epileptic treatment. *Life sciences,* 218**,** 314-323.

SABAPATI, M., PALEI, N. N., CK, A. K. & MOLAKPOGU, R. B. 2019. Solid lipid nanoparticles of Annona muricata fruit extract: formulation, optimization and in vitro cytotoxicity studies. *Drug development and industrial pharmacy,* 45**,** 577-586.

SELYUTINA, O. Y. & POLYAKOV, N. 2019. Glycyrrhizic acid as a multifunctional drug carrier–From physicochemical properties to biomedical applications: A modern insight on the ancient drug. *International Journal of Pharmaceutics,* 559**,** 271-279.

SIMON, A., DARCSI, A., KÉRY, Á. & RIETHMÜLLER, E. 2020. Blood-brain barrier permeability study of ginger constituents. *Journal of Pharmaceutical and Biomedical Analysis,* 177**,** 112820.

SOUTO, E. B., DOKTOROVOVA, S., ZIELINSKA, A. & SILVA, A. M. 2019. Key production parameters for the development of solid lipid nanoparticles by high shear homogenization. *Pharmaceutical development and technology,* 24**,** 1181-1185.

TETYCZKA, C., GRIESBACHER, M., ABSENGER-NOVAK, M., FRÖHLICH, E. & ROBLEGG, E. 2017. Development of nanostructured lipid carriers for intraoral delivery of Domperidone. *International Journal of Pharmaceutics,* 526**,** 188-198.

TETYCZKA, C., HODZIC, A., KRIECHBAUM, M., JURAIĆ, K., SPIRK, C., HARTL, S., PRITZ, E., LEITINGER, G. & ROBLEGG, E. 2019. Comprehensive characterization of nanostructured lipid carriers using laboratory and synchrotron X-ray scattering and diffraction. *European journal of pharmaceutics and biopharmaceutics,* 139**,** 153-160.

VAESSEN, S. F., VAN LIPZIG, M. M., PIETERS, R. H., KRUL, C. A., WORTELBOER, H. M. & VAN DE STEEG, E. 2017. Regional expression levels of drug transporters and metabolizing enzymes along the pig and human intestinal tract and comparison with Caco-2 cells. *Drug Metabolism and Disposition,* 45**,** 353-360.

VERTZONI, M., AUGUSTIJNS, P., GRIMM, M., KOZIOLEK, M., LEMMENS, G., PARROTT, N., PENTAFRAGKA, C., REPPAS, C., RUBBENS, J. & VAN DEN ABEELE, J. 2019. Impact of regional differences along the gastrointestinal tract of healthy adults on oral drug absorption: an UNGAP review. *European Journal of Pharmaceutical Sciences,* 134**,** 153-175.

YOSHIZATO, T., KOTEGAWA, T., IMAI, H., TSUTSUMI, K., IMANAGA, J., OHYAMA, T. & OHASHI, K. 2012. Itraconazole and domperidone: a placebo-controlled drug interaction study. *European journal of clinical pharmacology,* 68**,** 1287-1294.

ZHANG, J., WEN, X., DAI, Y. & XIA, Y. 2019. Mechanistic studies on the absorption enhancement of a self-nanoemulsifying drug delivery system loaded with norisoboldine-phospholipid complex. *International Journal of Nanomedicine,* 14**,** 7095.

ZHANG, X., XING, H., ZHAO, Y. & MA, Z. 2018. Pharmaceutical dispersion techniques for dissolution and bioavailability enhancement of poorly water-soluble drugs. *Pharmaceutics,* 10**,** 74.